

Optimization of Atmospheric Distillation Unit of Warri Refinery Using Artificial Neural Network and Exergy Rate Profiles

Funmilayo N. Osuolale^{1*} & Ambrose N. Anozie²

¹Ladoke Akintola University of Technology,
Ogbomoso, Oyo State, Nigeria
fnosuolale@lautech.edu.ng

²Covenant University,
Ota, Ogun State, Nigeria
ambrose.anozie@covenantuniversity.edu.ng

*Correspondence: fnosuolale@lautech.edu.ng

Abstract: In this paper, the operation of atmospheric distillation unit (ADU) of Warri refinery was optimized using Artificial Neural Network (ANN) method of optimization and exergy rate profiles (ERP). Optimization of ADU exergy efficiency using nine operating variables and ANN method of optimization improved exergy efficiency from 33% to 53%. The vapour and liquid exergy rate profiles in the distillation column were used to reveal points of inefficiency within the column and as a retrofit tool to suggest possible column modification alternatives for energy efficient operations. The exergy rate profiles in the column were found to be crossing each other. Optimization of the ADU when the crossing of the exergy rate profiles in the column was removed further improved ADU exergy efficiency from 53% to 60%. Artificial neural network was shown to be a powerful and suitable optimization method for solving constrained optimization problems such as in atmospheric distillation unit with several operating variables with constraints. Exergy rate profiles depict the driving forces between the liquid and the vapour states in a column and were shown to be a suitable tool for further improvement of ADU exergy efficiency.

Keywords: Atmospheric Distillation Unit; Artificial neural network; Exergy efficiency; Optimization; Exergy rate profiles

1. Introduction

Distillation process contrary to predictions of being replaced with some other separation techniques is still the most widely used separation process. The energy inefficiency of the process however, has always been the concern of researchers. This is because of the economic and environmental implications of unutilised energy [1]. The essential need of distillation system coupled with its demanding energy usage has led to a number of methods targeted at improving the effectiveness of the column. One of such methods is through the application of the laws of thermodynamics in the analysis of the column. This has been applied through pinch analysis and exergy analysis [2]. Pinch analysis is a synthesis tool. It shows in which way the heat can be added or extracted and it determines how best to place heating and cooling utilities for optimum energy performance. Pinch analysis is however, limited in its application to systems with heating or cooling requirement [3]. Exergy analysis on the other hand has a wide range of applicability but it is often used as a diagnostic tool to give an indication of how efficient a process is compared to its optimum possible performance [4] and to pinpoint regions of inefficiency in a column [5]. The challenge therefore, is to use exergy in the “how” of making a process efficient.

Diagrammatic representation of the thermodynamic analysis of distillation process has been used by a number of authors to give a better understanding as to what operates within the column. This is with a view to allow the designer or operator to identify useful modifications that will improve the efficiency and optimization of the column [6]. Dhole and Linhoff [7]

considered the column as a reversible column using temperature enthalpy profile in targeting for column modifications. The assumption of reversibility however, limits the application of this method to multicomponent mixtures and though the procedures led to column energy improvement, it does not identify the main sources of irreversibility within the column [8]. An attempt to overcome this deficiency in the thermodynamic analysis of the column led to introduction of the exergy loss profile [9]. Exergy loss profile could describe in a single variable the distribution of multicomponent heat and mass driving forces. It has been previously used in the retrofit of a crude distillation unit [10] and of recent in the optimization of operating parameters such as reflux ratio and feed stage [11]. However, considering the fact that distillation process is hinged on the transfer of mass and heat between two states (liquid and vapour), there is a need for a profile that will diagrammatically show this and as well provide means of improving the column based on the driving forces between the vapour and liquid states.

This present work is set to present exergy rate profiles for the column in atmospheric distillation unit (ADU) of Warri refinery. The exergy rate profiles serve as a tool to pinpoint the source of inefficiencies within the column and as a screening tool to determine retrofit options. The paper also presents exergy rate profiles as having a direct relation with the overall energy consumption of the column and hence shows a possibility to be used in optimizing the column without violating the specifications of the column. The paper is sectionalised as follows. Section 2 describes the Warri atmospheric

distillation unit under consideration. Section 3 gives the exergy analysis and exergy rate profiles concepts while section 4 gives the optimization procedures using Artificial Neural Network. Section 5 presents the results and discussion of the application and section 6 concludes the paper.

2. The System

The schematic diagram of the ADU of Warri Refinery is shown in Fig.1. It

operates above atmospheric pressure and is a long column that consists of 46 trays. The atmospheric residue is drawn from the bottom tray. The overhead vapours are condensed in the atmospheric column air cooler and collected in an accumulator. Both column bottom liquid and the liquid side cuts contain light ends. Light ends removal is achieved by injecting steam.

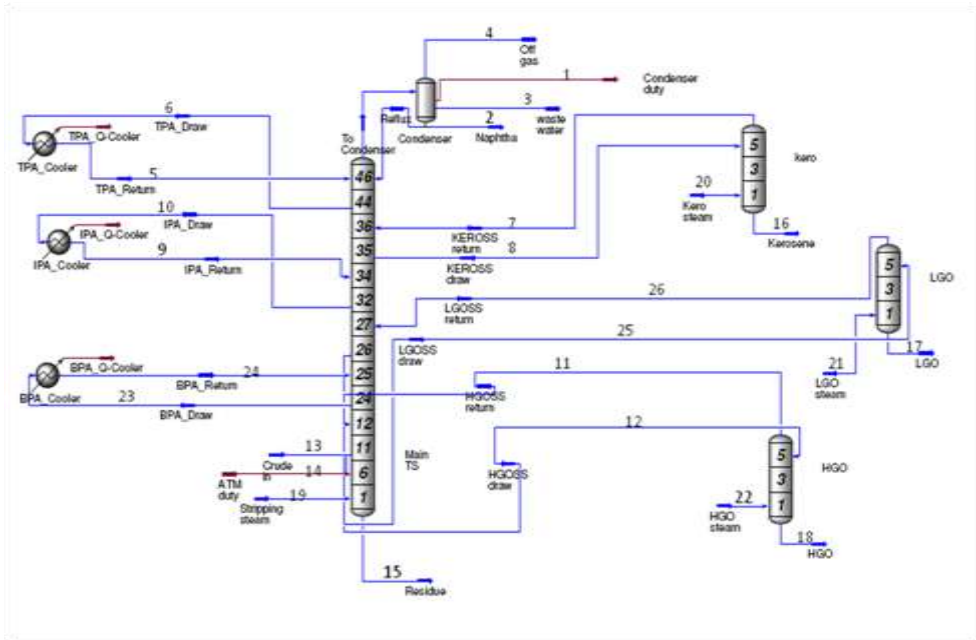


Figure 1: Schematic diagram of the Atmospheric Distillation Unit of Warri Refinery

Three side cuts are drawn respectively from the 35th, 26th and 11th trays and processed separately in the strippers. The kerosene cut is fed into the kerosene stripper above the 5th tray in the stripper, and vapours return to the main column above the 36th tray, while the stripped kerosene is sucked from the bottom of the stripper by a pump and sent to storage. The Light gas oil (LGO) cut is fed into the LGO stripper above the 5th tray in the stripper, and vapours return to main column above the 27th tray, while the stripped LGO is sent to

storage. The heavy gas oil (HGO) cut is fed into the HGO stripper above the 5th tray in the stripper, and vapours return to main column above the 12th tray. The top pump around (TPA), the intermediate pump around (IPA) and the bottom pump around (BPA) are drawn from tray 44, 32 and 24, respectively before being recycled back to the column after heat exchange.

3. Concepts of exergy and exergy rate profiles

3.1 Exergy analysis

Exergy is a concept from the first and second laws of thermodynamics and its calculation is based on the determination of the enthalpy and entropy of any given system. Usually the physical exergy of a system is calculated as [12]:

$$Ex_{ph} = m((h - h_0) - T_0(s - s_0)) \quad (1)$$

with the reference temperature given as 298K and the reference pressure as 1atmosphere. For chemical processes, the interaction between the chemical species in the system of study and the environmental precursors makes the calculation of the chemical exergy imperative. Different substances have different ways of chemical exergy calculation. For a crude stream which is of high interest here, standard molar chemical exergy is calculated from the standard molar chemical exergies of all identified components and pseudo-component as:

$$\Delta Ex_{ch} = \sum n_i b_{qi} + \sum n_i b_{chi} + RT_0 \sum n_i \ln a_i \quad (2)$$

where b_{chi} is the chemical exergy for component i ; b_{qi} is the chemical exergy for pseudo-component i ; and a_i is the activity coefficient of component i .

The standard chemical exergy for pseudo-components can be determined from heuristic empirical expression as a function of the elementary composition and their heating values [13]. This is calculated as:

$$B_{qi} = \varphi_i C_i \quad (3)$$

where φ_i is the regression equation determined to express the ratio H/C, N/C, O/C and S/C for the pseudo-components (H, C, N, O and S are elements – Hydrogen, Carbon, Nitrogen, Oxygen and Sulphur); C_i is the net calorific heating value of the pseudo-component i ; and

$$\varphi_i = 0.0401 + 0.1770 \frac{H_i}{C_i} + 0.0420 \frac{N_i}{C_i} + 0.0269 \frac{O_i}{C_i} \quad (4)$$

where z is compressibility factor. Total exergy of a stream is then calculated from the addition of the physical and chemical exergy of the stream.

Exergy losses in thermal process could be internal loss as a result of irreversible phenomena in the process plant or external loss as a result of waste products from the process. Major losses in the column are considered to be from internal losses. Hence the overall exergetic efficiency of the column is defined as:

$$\eta = \frac{\text{Exergy of useful products}}{\text{Exergy of feed}} \quad (5)$$

For the ADU, the exergetic efficiency was defined as:

$$\eta = \frac{\sum Ex_{out}}{\sum Ex_{in}} = \frac{Ex_{x16} + Ex_{x17} + Ex_{x18} + Ex_{x19} + Ex_{x20} + Ex_{x21} + Ex_{x22} + Ex_{x23} + Ex_{x24} + Ex_{x25} + Ex_{x26} + Ex_{x27} + Ex_{x28} + Ex_{x29} + Ex_{x30} + Ex_{x31} + Ex_{x32} + Ex_{x33} + Ex_{x34} + Ex_{x35} + Ex_{x36} + Ex_{x37} + Ex_{x38} + Ex_{x39} + Ex_{x40} + Ex_{x41} + Ex_{x42} + Ex_{x43} + Ex_{x44} + Ex_{x45} + Ex_{x46} + Ex_{x47} + Ex_{x48} + Ex_{x49} + Ex_{x50} + Ex_{x51} + Ex_{x52} + Ex_{x53} + Ex_{x54} + Ex_{x55} + Ex_{x56} + Ex_{x57} + Ex_{x58} + Ex_{x59} + Ex_{x60} + Ex_{x61} + Ex_{x62} + Ex_{x63} + Ex_{x64} + Ex_{x65} + Ex_{x66} + Ex_{x67} + Ex_{x68} + Ex_{x69} + Ex_{x70} + Ex_{x71} + Ex_{x72} + Ex_{x73} + Ex_{x74} + Ex_{x75} + Ex_{x76} + Ex_{x77} + Ex_{x78} + Ex_{x79} + Ex_{x80} + Ex_{x81} + Ex_{x82} + Ex_{x83} + Ex_{x84} + Ex_{x85} + Ex_{x86} + Ex_{x87} + Ex_{x88} + Ex_{x89} + Ex_{x90} + Ex_{x91} + Ex_{x92} + Ex_{x93} + Ex_{x94} + Ex_{x95} + Ex_{x96} + Ex_{x97} + Ex_{x98} + Ex_{x99} + Ex_{x100}}{Ex_{x1} + Ex_{x2} + Ex_{x3} + Ex_{x4} + Ex_{x5} + Ex_{x6} + Ex_{x7} + Ex_{x8} + Ex_{x9} + Ex_{x10} + Ex_{x11} + Ex_{x12} + Ex_{x13} + Ex_{x14} + Ex_{x15}} \quad (6)$$

The exergetic efficiency of the side strippers were also calculated as:

$$\eta_{s1} = \frac{Ex_{x26} + Ex_{x17}}{Ex_{x25} + Ex_{x21}} \quad (7)$$

$$\eta_{s2} = \frac{Ex_{x11} + Ex_{x18}}{Ex_{x12} + Ex_{x22}} \quad (8)$$

$$\eta_{s3} = \frac{Ex_{x7} + Ex_{x16}}{Ex_{x8} + Ex_{x20}} \quad (9)$$

where η_{s1} , η_{s2} , and η_{s3} are efficiencies for LGO, HGO and Kerosene side strippers. The numbers are representing the streams as given in Figure 1. Irreversibility, I , was also calculated as:

$$I = \sum Ex_{in} - \sum Ex_{out} \quad (10)$$

3.2 Exergy rate profiles

The calculation of exergy rates for each stage in the liquid and vapour states for binary distillation system has been reported earlier [14, 15] and is now being applied to multicomponent distillation system. It is calculated for the liquid and vapour states of each tray as:

$$\Delta Ex_{tray} = \Delta H - T_0 \Delta S \tag{11}$$

$$\begin{aligned} Ex_{iL} &= (h_{iL} - h_{0iL}) - T_0 (s_{iL} - s_{0iL}) \\ Ex_{iV} &= (h_{iV} - h_{0iV}) - T_0 (s_{iV} - s_{0iV}) \end{aligned} \tag{12}$$

where Ex_{iL} is exergy of liquid stream of tray i ; h_{iL} is enthalpy of liquid stream of tray i ; F_{iL} is liquid flow rate of tray i ; h_{0iL} is enthalpy of liquid stream of tray i at reference conditions; T_0 is the reference temperature = 298.15 K; s_{0iL} is the entropy of liquid stream of tray i at reference conditions; and s_{iL} is the entropy of liquid stream for tray i , and is given by the equation 13:

$$s_{iL} = h_{iL} \frac{\left(\ln \frac{T_i}{T_0} - R \ln \frac{P_i}{P_0} \right)}{T_i - T_0} \tag{13}$$

where T_i = Temperature of tray i ;
 P_i = Pressure of tray i ; R = Gas constant = 8.314kJ/kmolK; P_0 = 101.3kPa.

Similarly, the vapour stream equations are:

$$Ex_{iV} = (h_{iV} - h_{0iV}) - T_0 (s_{iV} - s_{0iV}) = \Delta H_{iV} - T_0 \Delta S_{iV} \tag{14}$$

$$s_{iV} = h_{iV} \frac{\left(\ln \frac{T_i}{T_0} - R \ln \frac{P_i}{P_0} \right)}{T_i - T_0} \tag{15}$$

Exergy rate profiles are therefore a plot of tray number versus exergy of liquid state (Ex_{iL}) and exergy of vapour state (Ex_{iV}).

4. Optimization procedures using Artificial Neural Network

4.1 Model Formulation

The model building process was done in four sequential steps, namely: Data processing, Network creating, Network training and testing, and Analysis of the network performance. Neural network training can be made more efficient when certain preprocessing steps are performed on the network inputs and targets. Network-input processing functions transform inputs into a better form for the network use. Post-processing steps transform outputs back to the characteristics of the original target data. The function “Mapminmax” was used to scale the inputs and targets so that they always fall within a specified range before training began. The “Newff” network function which creates a feed forward back propagation network was used. “Trainlm” is the network training function that was used. The networks were trained using supervised learning algorithm. The Levenberg-Marquardt back-propagation learning algorithm was used. The algorithm divides the data into three partitions, namely: the training data set, the test data set and validation data set. 80% of the data was used for the training data, 10% for the testing and the remaining 10% for the validation. The training data set is for the training purposes; the test data is to check the generalization performance of the trained neural network model. The training was stopped when the performance on the test data set results into minimum model error. The validation data set is to validate the model. The performance function used was the mean square estimate (MSE). It measures the network performance

according to the mean of squared errors given in equation (16).

$$MSE = \frac{1}{Q} \sum_{k=1}^Q [T_i(k) - a(k)]^2 \quad (16)$$

A flow chart depicting the processes involved in the modelling is shown in Figure 2.

4.2. Genetic algorithm optimization

The genetic algorithm is a method for solving both constrained and unconstrained optimization problems that is based on natural selection, the process that drives biological evolution. The genetic algorithm repeatedly modifies a population of individual solutions. At each step, the genetic algorithm selects individuals at random from the current population to be

parents and uses them to produce the children for the next generation. Over successive generations, the population "evolves" toward an optimal solution. The genetic algorithm (GA) uses three main types of rules at each step to create the next generation from the current population:

- i. Selection rules select the individuals, called parents that contribute to the population at the next generation.
- ii. Crossover rules combine two parents to form children for the next generation.
- iii. Mutation rules apply random changes to individual parents to form children.

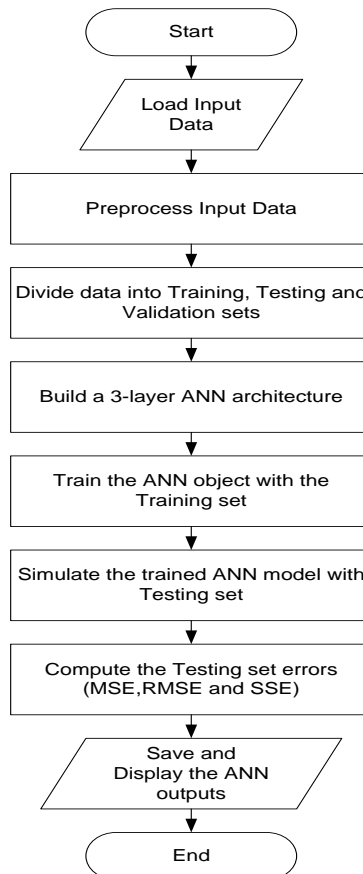


Figure 2: Simulation flow chart of the neural network

The GA optimization problem of the ADU can be stated as:

$$\text{Max } f(x, m, y) \quad (17)$$

$$x_a \leq x \leq x_b$$

$$y = U(x, m)$$

where f is the objective function; x is the controllable variables; m is the uncontrollable variables; y is the efficiency of the column; U is the knowledge database (neural network model) of the crude distillation system; and the notation of a and b represent the lower bound and the upper bound, respectively.

5. Results and Discussion

5.1 Exergy analysis

Table 1 shows the state parameters for the refinery simulation and the material streams that were considered in the analysis. The results of the analysis for the refinery are given in Table 2. The physical exergy efficiency of the ADU is 33.27% with an irreversibility of 4.2×10^8 kJ/h while the total exergy efficiency (physical + chemical) is 33.34%. Here the contribution of the chemical exergy to the efficiency is insignificantly low (0.07%). The low value might result from the lack of chemical reaction taking place in the column. The distillation process is basically a physical operation resulting

from the differences in boiling points of components in the process. A reactive distillation process will have a higher level of contribution from chemical exergy.

The low efficiency of the ADU is suggesting a serious need for improvement of the column for better energy utilisation. The operation of a distillation unit involves the use of a high exergy content steam that is ejected in a low temperature condenser. The area of concentration for the improvement of the process will therefore be on the column. This is attested to from the efficiencies of the side strippers as listed in Table 2. The efficiencies in percentages are 93.93, 94.40 and 87.52 for KERO, LGO and HGO side strippers, respectively.

The energy efficiency of the ADU is 86.48%. This is far apart from the exergy efficiency result. It has been confirmed that efficiency of processes is better analysed using the second law of thermodynamics rather than the first law. The overall exergy efficiency of the unit (ADU+Prelash) is 3.64%. The contribution of ADU to this inefficiency is greater and much work should be concentrated on the ADU for the overall improvement of the unit.

Table 1: Material streams parameters from the simulation of the Atmospheric Distillation Unit

Stream No	Stream Name	Temperature (°C)	Pressure (kPa)	Molar Flow (kgmol/h)
2	Naphtha	184.3	45	3387
3	Waste water	184.3	45	0.0000
4	Off gas	184.3	45	7106
5	TPA return	164	50.2	8284
6	TPA draw	232	50.2	8284

7	KEROSS draw	258	70.48	164.2
8	KEROSS return	264.1	70.48	2090
9	IPA return	207.1	77.4	1.373e4
10	IPA draw	275.1	77.4	1.373e4
11	HGOSS return	323.5	124.6	90.90
12	HGOSS draw	332.5	124.6	518.4
13	Crude in	350	156.9	1.914e4
15	Residue	324.8	147.1	3455
16	Kerosene	243.6	70.48	1962
17	LGO	277.3	90.76	3123
18	HGO	296.5	103.4	455.7
19	Stripping steam	151.8	500	95130
20	Kero steam	151.8	186.3	36.08
21	LGO steam	151.8	205.9	83.26
22	HGO steam	151.8	225.6	27.75
23	BPA draw	308.4	95.27	6233
24	BPA return	278.5	95.27	6233
25	LGO draw	300.7	90.76	3378
26	LGO return	293.8	90.76	3378

Table 2: Efficiency Calculations for ADU base case

	Exergy Efficiency (%)	Energy Efficiency (%)	Irreversibility (kJ/h)
ADU	33.27	86.48	4.179×10^8
LGO	94.40	≈ 100	2.56×10^6
HGO	87.52	≈ 100	1.149×10^6
KERO	93.93	≈ 100	1.18×10^6

5.2 Exergy Rate Profiles

Distillation process is hinged on the principle of heat and mass transfer between the liquid and the vapour state on a stage by stage level. The in-depth study of states' interaction on each stage is therefore necessary. The exergy rate profile simultaneously describes the first and second laws of thermodynamics on a single diagram and hence gives a better insight between the liquid and the vapour state. The exergy rate profiles show the distribution of driving forces within the column between the liquid and the vapour states of each tray. The profiles equally show the feasibility of the column design. A crossing of the profiles is thermodynamically infeasible and connotes an infeasible design [14, 15].

In Figure 3, a crossing of the profiles is noticed showing that there are points within the column when the exergetic liquid phase flow is higher than the vapour flow and creating pinch points that are contributing to the inefficient performance of the column. Exergy rate profiles are calculated putting temperature and mass flow of the phases under consideration; there are no temperature and mass transfer driving

forces at these points of crossing. These are indicators of sources of inefficiency within the column. Exergy rate profiles can be used for targeting possible ways of column modifications right at the design stage.

Usually, ways of reducing dissipated energy in processes is to increase the process reversibility by increasing equipment size. A better way however will be to localise the energy supplied within the process by distributing the driving force evenly and exergy rate profile will give an indication of whether this has been achieved and hence, instilling confidence for an efficient design or stimulating the designer for a better column performance.

A marked difference is noticed on the sixth stage. This stage is the feed stage of the refinery. This is indicating some other factors that are contributing to the inefficiency of the column. The feed conditions of the refinery might not be adequate. The inappropriate feed condition causes a sharp change in the exergy rate profiles near the feed stage. This is in line with the work of Dhole and Linnhoff [7] on the use of column grand composite curve (CGCC) for column modifications. The sharp rise in

the vapour profile suggests an excessive heat supply for the feed stage and ultimately an unnecessary condenser load. Exergy rate profiles make it easy to see a feed which is excessively heated or subcooled and hence, minimises the condenser and reboiler load. However, because of the fact that there is a limit at which the inlet temperature of the crude can be raised to prevent cracking [16] and considering the reality that the ratio of the crude to the stripping steam is less than that suggested in the literature (5-10%), the line of increasing steam flow rate may be considered. The exergy rate profiles also show modification for side condensing/reboiling of the column. The kinked nature of the liquid phase curves occurred in the column at the tray where pump around flow are

returned to the column. This kinked nature is suggesting modifications for the pump around flow for an efficient design.

Attempts were made to remove the crossing of the profiles by altering the feed condition and the stripping steam flow rate. The result is given in Figure 4. If the kinked nature of the profiles is removed and there is a reduction in the driving force, it will give a much higher efficiency. Another way is to consider optimizing the column operating conditions for the optimum combinations of the operating parameters that will result in exergy rate profiles not crossing each other with the column efficiency being the objective function. This was explored next using expert system.

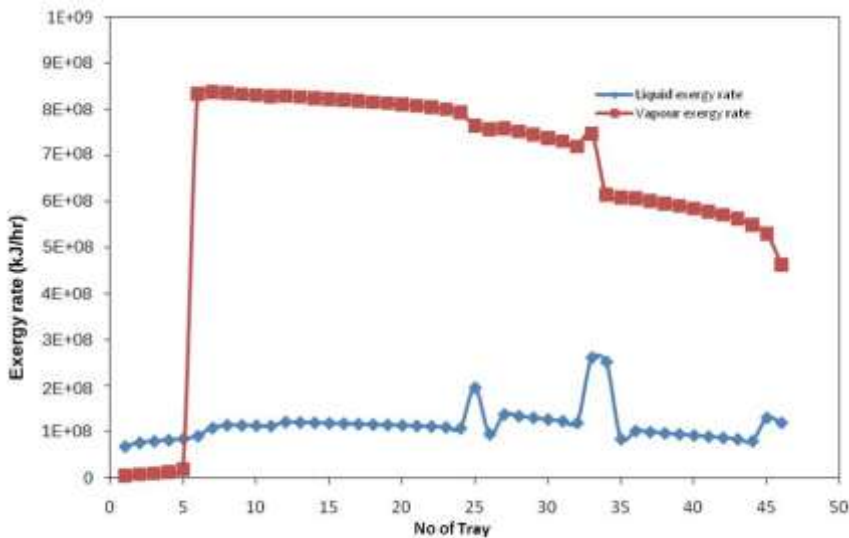


Figure 3: Exergy rate profile for Warri ADU base case

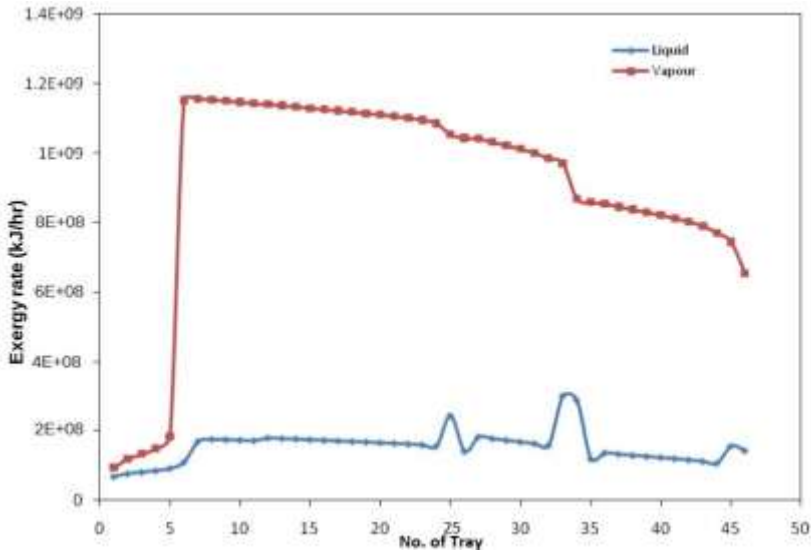


Figure 4: Exergy rate profile for Warri ADU (Crossing removed)

5.3 Neural Network Model

The NN model was trained to represent the knowledge data base of the ADU operating system using the ADU simulated runs from HYSYS. Two thousand and thirty four (2034) data sets were used in training the ADU for the refinery. 10% of the data set was used to test the trained model. The result of comparison between the real/actual data output and the target output from the model shows that the models predict the actual data accurately. Liao et al. [17] and Motlaghi et al. [18] obtained similar result though their data were basically experimental.

The correlation coefficient of the ANN model was 0.9999. This implies that the relative error of the trained model and the tested data was below 1×10^{-4} , showing that the NN model was quite reliable in describing the input-output relationship of the ADU. The NN model was able to adequately represent

the complex process of the ADU due to the non-linear characteristics of the NN structure. Figure 5 also illustrate the best linear regression fit of the output and the target data of the refineries which in each case approaches 1. The validation performance parameter is 0.0010531. All these are good indicators that the trained models for the refineries predict accurately. The models therefore can be used to determine the outcome of changes in any of the given input parameters; it can correlate the relationship between the input and output variables of the refinery. It can also predict and point out the effects of the operating variables on the products of the refinery as well as the efficiency of the ADU. This will either serve as stimuli to operators that the operating conditions are ideal for an efficient column or as impetus that better combinations of operating conditions can be searched for.

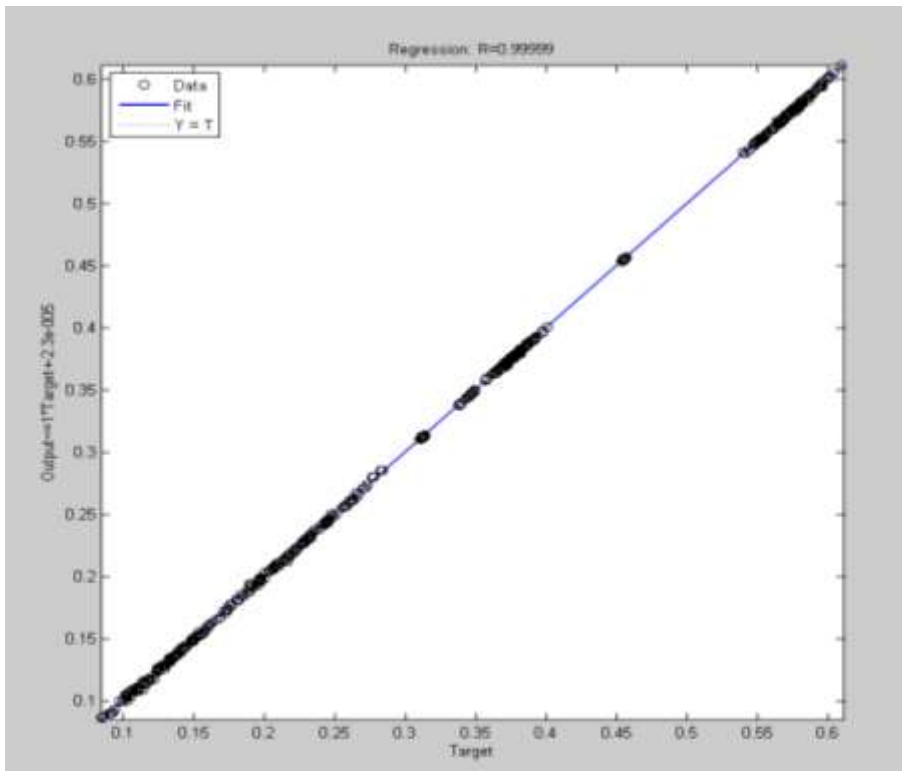


Figure 5: Correlation between the NN predicted values and simulated

5.4 Genetic algorithm optimization

The genetic optimization was done for the existing operating conditions of the refineries and the operating conditions resulting from the exergy rate profile. The optimization problems here consist of an objective function to be maximised together with constraints from design and operation conditions. The objective function is the exergy efficiency, subject to the constraints of the given controllable variables with the following upper and lower boundaries:

- $300 \leq \text{Feed temperature} \leq 360$
- $3e4 \leq \text{Steam mass flow} \leq 1e5$
- $220 \leq \text{Steam temperature} \leq 260$
- $5434 \leq \text{TPA rate} \leq 1.09e5$
- $2.1e4 \leq \text{IPA rate} \leq 5.43e4$
- $1.63e4 \leq \text{BPA rate} \leq 1.41e5$
- $86.4 \leq \text{TPA}\Delta T \leq 176.4$
- $68.4 \leq \text{IPA}\Delta T \leq 158.4$

$$86.4 \leq \text{BPA}\Delta T \leq 176.4$$

Thus a total of nine process variables were used for the optimization. The knowledge database of the neural network model was used in the optimization procedures. About 100 generations were made and the output with the least error was returned as optimum. The corresponding efficiency for these combinations was 53%. This is a great improvement from an initial efficiency of 33%. The optimum input from the optimization procedures were also validated in HYSYS and the efficiency was close to that predicted. The expert system can be said to adequately predict the optimum conditions at which the ADU can operate with the least irreversibility. The operating conditions that led to the removal of the crossing were also

optimised and a new set of optimum conditions that give a non-crossing exergy rate profiles were found. The efficiency at this point was 60% showing a marked increase of 7% to the optimum efficiency when the exergy rate profiles were not considered. The exergy rate profile which gives feasible thermodynamic conditions of the column also gives a higher thermodynamic efficiency and hence it's a preferred method of column optimization. Table 3 gives the base case operating conditions, the optimum operating conditions for the base case

and the optimum operating conditions for the exergy rate profiles (ERP) modified case.

6. Conclusion

Artificial neural network method of optimization afforded the means of using up to nine operating variables in optimizing the operation of an atmospheric distillation unit in a crude distillation unit of a refinery which resulted in a 20% increase in exergy efficiency. Exergy rate profiles were calculated putting temperature and mass flow rates of the

Table 3: Comparison between base case, optimum values of the base case and ERP modified case

	Base case	Optimum base case	Optimum ERP modified
Feed temperature °C	350	300	307
Steam flow Kg/h	5285	4183	7226.4
Steam Temperature	151.8	231	232
TPA rate barrel/day	1250	7747	6164
IPA rate barrel/day	2072	85044	21807
BPA rate barrel/day	9409	38640	84424
TPAΔT °F	154	109	92
IPAΔT °F	154	79	73
BPAΔT °F	86	134	131
Efficiency %	33	53	60

phases into consideration. When the profiles cross each other there are no temperature and mass transfer driving forces at these points of crossing. These are indicators of sources of inefficiency within the column. The exergy rate profiles revealed the source of

inefficiency within the column. It was used to target possible ways of column modifications. The crossing of the profiles was removed and it further improved the exergy efficiency of the column by 7%.

References

1. M.A. Rosen and I. Dincer, "On exergy and environmental impact," *International Journal of Energy Research*, 21(7), pp. 643-654, 1997.
2. Y. Demirel, "Thermodynamic analysis of separation system," *Separation Science and Technology*, 39, pp. 3897-3942, 2004.
3. M.A. Gadalla, O.Y. Abdelaziz and F.H. Ashour, "Conceptual insights to debottleneck the network pinch in heat integrated crude oil distillation systems without topology modifications", *Energy Conversion and Management*, Volume 126, pp 329-341, 2016
4. A. Doldersum, "Exergy analysis proves viability of process modifications," *Energy Conversion and Management*, 39(16-18), pp. 1781-1789, 1998.
5. S.F. Wang, T. Ma, G. Gao, P. Wu and L. Liu, "Energy and exergy analysis of a five-column methanol distillation scheme." *Energy*, Volume 45, Issue 1, pp. 696-703, 2012.
6. R.J. Zemp, S.H.B. de Faria and M.d.L. Oliveira Maia, "Driving force distribution and exergy loss in the thermodynamic analysis of distillation columns," *Computers & Chemical Engineering*, 21, Supplement, pp. S523-S528, 1997.
7. V.R. Dhole and B. Linnhoff, "Distillation column targets," *Computers & Chemical Engineering*, 17(5-6), pp. 549-560, 1993.
8. R. Smith and R.J. Zemp, (eds.) *Process integration of separation systems* Rugby, UK: IChemE. 1994.
9. S.H.B. Faria and R.J. Zemp, "Using exergy loss profiles and enthalpy-temperature profiles for the evaluation of thermodynamic efficiency in distillation columns," *Thermal Engineering*, 4, pp. 76-82, 2005.
10. A.H. Tarighaleslami, M.R. Omidkhan, A. Ghannadzadeh and R.H. Hesas, "Thermodynamic evaluation of distillation columns using exergy loss profiles: a case study on the crude oil atmospheric distillation column," *Clean Technologies and Environmental Policy*, 14(3), pp. 381-387, 2012.
11. L.B. Rocha, M.L. Gimenes, S. Farai, L. Jimenez and T. Cavali, "A new methodology to reduce exergy loss of distillation columns using rigorous process simulation," *Computer Aided Chemical Engineering*, Volume 38, pp. 1003-1008, 2016.
12. J. Szargut, D.R. Morris and F.R. Steward, *Exergy analysis of thermal, chemical and metallurgical processes*. New

- York: Hemisphere Publishing Corporation, 1998.
13. R. Rivero, C. Rendon and L. Monroy, "The Exergy of Crude Oil Mixtures and Petroleum Fractions: Calculation and Application," *International Journal of Thermodynamics*, 2(3), pp. 115-123, 1999.
 14. A.N. Anozie, A.S. Osunleke and T.C. Aseeperi, "Exergy analysis and optimisation of binary plate distillation column operations," *International Journal of Exergy*, 7, pp. 593-606, 2010.
 15. A.N. Anozie, F.N. Osualale and A.S. Osunleke, "Exergy analysis of binary plate distillation column operations," *International Journal of Exergy*, 6, pp. 715-728, 2009.
 16. J.H. Gary and G.E. Handwerk, *Petroleum refining*. Taylor and Francis, 2001.
 17. S. Motlaghi, F. Jalali and M.N. Ahmadabadi, "An expert system design for a crude oil distillation column with the neural networks model and the process optimization using genetic algorithm framework," *Expert systems with applications*, volume 35(4), 1540-1545, 2008.
 18. L.C. Liau, T.C. Yang, and M. Tsai, "Expert system of a crude oil distillation unit for process optimization using neural networks," *Expert systems with applications*, volume 26(2), 247-255, 2004.